

Supporting Information

Highly Stretchable Ionic Hydrogels with Enhanced Thermoelectric Performance and Flame Retardancy for Intelligent Fire Protection

Mi Fu^{a,†}, *Zhengzhong Wu*^{b,†}, *Xiaobo Liu*^a, *Yuwei Yuan*^a, *Xuejun Lai*^{b,*}, *Kan Yue*^{a,c,*}

^aGuangdong Basic Research Center of Excellence for Energy and Information Polymer Materials, South China Advanced Institute for Soft Matter Science and Technology, School of Emergent Soft Matter, South China University of Technology, Guangzhou 510640, China

^bKey Lab of Guangdong Province for High Properties and Functional Polymer Materials, School of Materials Science and Engineering, South China University of Technology, Guangzhou 510640, China

^cJiangsu Province Cultivation base for State Key Laboratory of Photovoltaic Science and Technology, Changzhou University, Changzhou, 213164, Jiangsu, China

*Corresponding author, E-mail: kanyue@scut.edu.cn (K. Yue); E-mail: msxjlai@scut.edu.cn (X. Lai)

†M. Fu and Z. Wu contributed equally to this work.

Experimental Section

Materials

Poly (ethylene oxide) (PEO) with average molecular weight $M_w = 100000$ kg/mol was obtained from Acros. Acrylic acid (98.0%, AA), 2-hydroxy-4'-(2-hydroxyethoxy)-2-methylpropiophenone (98.0%, Irgacure 2959), and sodium dihydrogen phosphate (98.0%, SDP) were obtained from Adamas-beta® (Co., Ltd., China).

Synthesis of the PAA-PEO-SDP Ionic Hydrogels

The PAA-PEO-SDP ionic hydrogels were prepared by the one-pot photo-initiated free radical polymerization process. In order to prepare the prepolymer solutions, PEO (5.35 g, 1 equiv., 0.0535 mmol), AA (5 ml, 1 equiv., 0.0321 mmol), sodium dihydrogen phosphate (SDP) of different concentrations, and photo-initiator Irgacure 2959 (0.1 g) were dissolved in 15.7 ml deionized (DI) water and stirred overnight to form a clear solution. The prepolymer solution was placed in a vacuum defoaming apparatus for around 5 min to remove the bubbles, and then moved into a closed glass mold coated by two polyethylene terephthalate (PET) substrates in the glove box under nitrogen atmosphere. The precursor solution was polymerized under UV light (365 nm, 72 W) for 1 h to afford the PAA-PEO- x MSDP ionic hydrogel ($x = 0.1, 0.2, 0.3$).

Morphology Characterization

The morphology change and elements mapping were tested by Scanning electron microscopy and energy dispersive X-ray spectrometry (SEM-EDS) (JSM-7900F, JEOL, Japan).

FTIR Characterization

The Fourier-transform infrared spectroscopy (FTIR) test was performed on an infrared spectrometer (FT/IR-4X, JASCO, Japan) using the attenuated total reflection (ATR) mode.

Mechanical Characterization

Tensile testing and compressive testing were performed on an electronic tensile machine (LD22.102 instrument, LiShi, Shanghai, China) with a 100 N load cell in an ambient condition (25 °C). The elastomer samples were cut into a dumbbell shape with a dimension of $2 \times 35 \times 1.0$ mm³ and the tensile testing were recorded at a speed of 100 mm/min. In a compressive testing, the sample is made into the original sheet with a diameter of 8 mm and a thickness of about 2 mm, and the cyclic compressive tests were recorded using a 100 N load cell at a constant speed of 1 mm/min with a strain of 90%.

Rheological Characterization

Rheological properties were measured by the ARES-G2 rheometer (TA Instruments, New Castle, DE, USA) equipped with a 25 mm diameter plate and a 0.9 mm plate-to-plate distance. To measure the linear viscoelastic region, the amplitude sweep rheological analyses were evaluated at a constant angular frequency of 1 Hz with the strain range of 0.1-200%. To measure the G' and G'' values, the frequency sweep rheological analyses were evaluated in the linear viscoelastic region at a constant strain of 5% with angular frequency range of 100-0.1 rad/s.

Electrical Characterization

The electrical characterization of the hydrogels was performed on an electrochemical workstation (CHI660e, CH Instruments, USA). The impedance is measured by the EIS method. The initial voltage was the measured open voltage; the frequency ranged from 1 Hz to 1 MHz; and the AC amplitude was 0.01 V. The ionic conductivity was measured using thin film samples with dimensions of $10 \times 10 \times 1 \text{ mm}^3$. Two ends of the sample were clamped with stainless steel discs, leaving 1 mm ionic conduct distance (L) in the middle. Then the Nyquist plot of the hydrogels can be obtained by this method. The following formula is used to calculate the ionic conductivity:

$$\sigma = L/RS,$$

where σ is the ionic conductivity, L is the thickness of the sample, R is bulk resistance of the sample obtained from the Nyquist plot and area of the sample. Conductivity experiments at different temperatures were carried out using a self-built temperature control device.

Thermal-electrical Characterization

The short-circuit voltage and short-circuit current of the sample under the given temperature difference are measured by the digital source meter (2450, Keithley Instruments, Inc., USA). The ionic hydrogels samples are made into a block of $15 \times 15 \times 2.5 \text{ mm}^3$ and the upper and lower surfaces are covered with the platinum electrode of 0.1 mm thick.

Thermal Conductivity Characterization

The thermal conductivity of the samples was measured by the transient hot-wire method using a thermal conductivity instrument (TC 3000E, XIATECH, China). The experimental voltage is 1V, and the acquisition time is 5 seconds. Each hydrogel sample was made into a block of $20 \times 30 \times 3 \text{ mm}^3$, two blocks are required for each concentration from 0M to 0.3M. The measurement was repeated at least 5 times, and the average value is determined.

Thermogravimetric analysis (TGA)

Thermogravimetric analyzer (TG209F1, Netzsch, Germany) was used to measure the thermogravimetric curves of the samples in air atmosphere from 35 to 800 °C at a heating rate of 20 °C min⁻¹.

Thermogravimetry-Fourier transform infrared spectrometry (TG-FTIR)

The TG-FTIR was performed on a thermogravimeter (SFPA 449C, Netzsch, Germany) connected with an infrared spectrometer (Tensor 27, Bruker, Germany). The spectra were recorded in air atmosphere from 30 to 800 °C, and the heating rate was 20 °C min⁻¹.

Flame retardancy Characterization

The limiting oxygen index (LOI) test was performed on a JF-3 oxygen index meter (JF3, Nanjing Jiangning Analytical Instrument, China) based on ASTM D2863-09, with the sample size of 70 mm × 10 mm × 10 mm.

The vertical burning test was carried out on SF-2 and MCSF-8 by a propane lamp with the sample size of 50 mm × 10 mm × 10 mm according to ANSI/UL 94-2010. The distance between the wick and the bottom of the spline is about 20 mm. After the spline is burned on the flame for 30 s, the flame is removed. The ignition is repeated and the burning state of the spline is observed and recorded.

Microscale Combustion Calorimeter (MCC) performed by a microcalorimeter (Govmark MCC-3, Deatak, US) based on ASTM D7309. Samples (10-12 mg) were tested at a heating rate of 1 °C/min from 25 to 600 °C.

Fire-warning test

The samples (50 mm × 10 mm × 2 mm) were connected to a millivolt signal alarm (HB414, Dongguan Daxian Instrument Equipment Co., Ltd., China) and a digital multi-meter (DMM6500 6 1/2, Keithley Instrument, USA). Copper foil was used as electrode, whose length at both ends of the sample was 5 mm. Sample was burned by an alcohol lamp flame with a length of 40 mm (the distance between the bottom of the sample and the wick was about 20 mm, and the flame was 20 mm away from one end) and the trigger voltage was set as 50 mV. Then, a camera was used to record the entire fire-warning test.

X-ray photoelectron spectroscopy (XPS)

X-ray photoelectron spectroscopy (XPS) was performed on an X-ray photoelectron spectrometer (Axis Ultra DLD, Kratos, Britain). The acceleration voltage and current were 15 kV and 5 mA, respectively, and the beam spot size was 700 μm × 300 μm.

Table S1-S4.**Table S1.** Compositions and contents of the PAA-PEO-*x*MSDP ionic hydrogels.

Concentration of SDP	PEO /g	AA /ml	I2959 /g	Water /g	SDP /g	MBAA /mg
0M	5.35	5	0.1	15.7	0	2.5
0.1M	5.35	5	0.1	15.7	0.188	2.5
0.2M	5.35	5	0.1	15.7	0.377	2.5
0.3M	5.35	5	0.1	15.7	0.565	2.5

Table S2. Specific values and average values of thermal conductivity of PAA-PEO-SDP ionic hydrogels with different SDP contents at room temperatures.

Sample Number	0M	0.1M	0.2M	0.3M
1	0.4487	0.4514	0.4452	0.4456
2	0.4465	0.4512	0.4471	0.4458
3	0.4456	0.4472	0.4421	0.4457
4	0.4475	0.4463	0.4418	0.4431
5	0.4415	0.4431	0.4411	0.4442
Average	0.4459	0.4478	0.4434	0.43312

Table S3. Micro calorimetric characteristic parameters of PAA-PEO-0M/0.3MSDP ionic hydrogels.

Sample	HR Capacity ($J \cdot g^{-1} \cdot K^{-1}$)	PHRR ($W \cdot g^{-1}$)	THR ($kJ \cdot g^{-1}$)	Temperature ($^{\circ}C$)	UL-94 rating
0M	393	337	22	396	V-1
0.3M	171	173	10	445	V-0

Table S4. Comparison of PAA-PEO-SDP and other thermoelectric type intelligent flame-retardant materials.

Materials	Seebeck Coefficient (mV K ⁻¹)	Ionic conductivity (mS cm ⁻¹)	Self-extinguishing time (s)	Stretchability (%)	LOI (%)	Trigger conditions ^a	Trigger time (s)	Trigger rate (mV s ⁻¹)	Ref.
PAA-PEO-SDP	24.7	1.7	<1	4270	54	>50 mV	1.5	33.4	This work
HTIG	3.4	11.6	<1	377	>80	>50 mV	4.0	12.5	[S1]
PILGs	1.3	13.3	<1	-	45	>50 mV	1.1	45.4	[S2]
CF-TE-FR	-	-	2	-	-	>5 mV	0.8	6.3	[S3]
CF-CP-FR	0.011	-	<1	-	-	>5 mV	1.0	5.0	[S4]
MAA e-textile	0.014	-	<1	-	-	>1 mV	1.6	0.6	[S5]
MFNC	0.008	-	<1	-	40	>1 mV	3.1	0.3	[S6]
HTE@CF	0.039	-	<1	-	35	>2 mV	3.0	0.7	[S7]
MXene/CCS	0.010	-	>3	-	46	>1 mV	3.8	0.3	[S8]
TE-FR100	0.020	-	<1	-	42	>1 mV	2.8	0.4	[S9]
PMA	0.008	-	<1	-	53	>1 mV	4.0	0.3	[S10]
PEDOT:PSS/SWCNT	0.9	-	<1	-	-	>1 mV	3.0	0.3	[S11]
PPy-CS/MXene	0.013	-	<1	-	31	>1 mV	1.9	0.5	[S12]

a. Trigger conditions: conditions required for the signal detection device to trigger the alarm.

Fig. S1-S14.

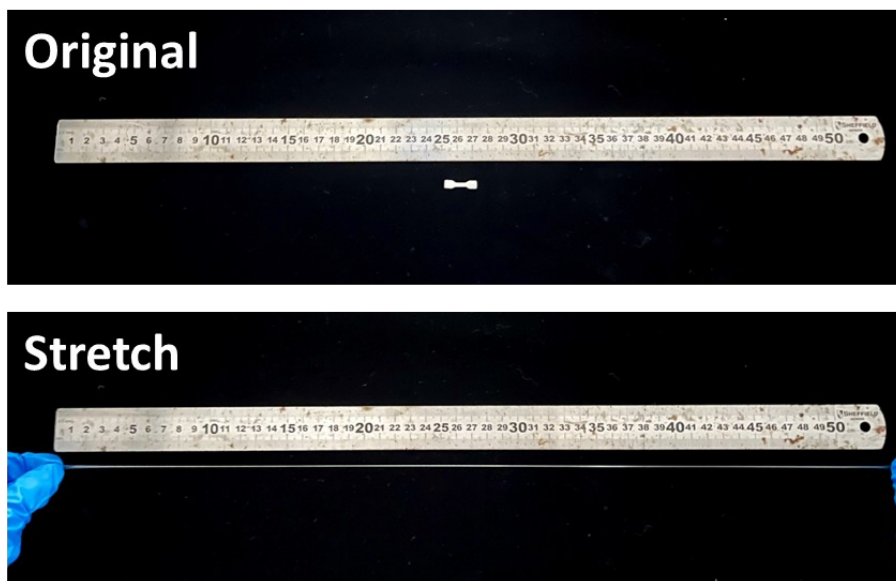


Figure S1. Photographs of the ionic hydrogels captured original and after stretching.

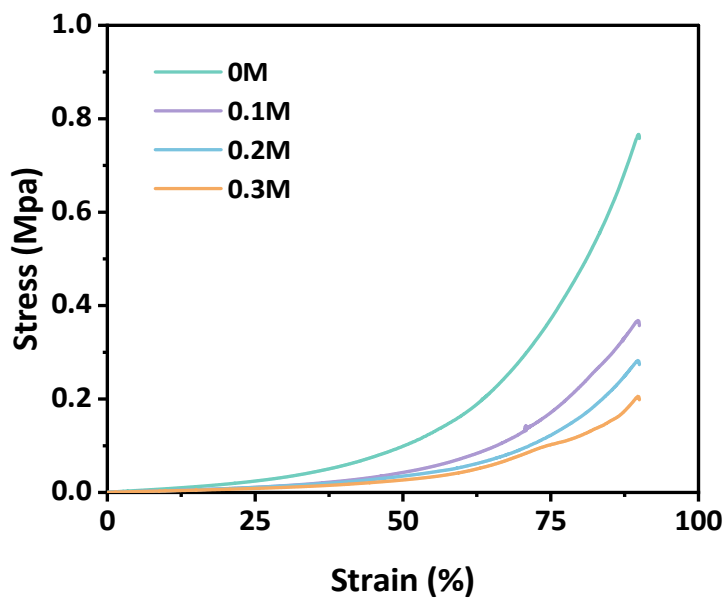


Figure S2. Compressive stress-strain curves of ionic hydrogels at different SDP concentrations.

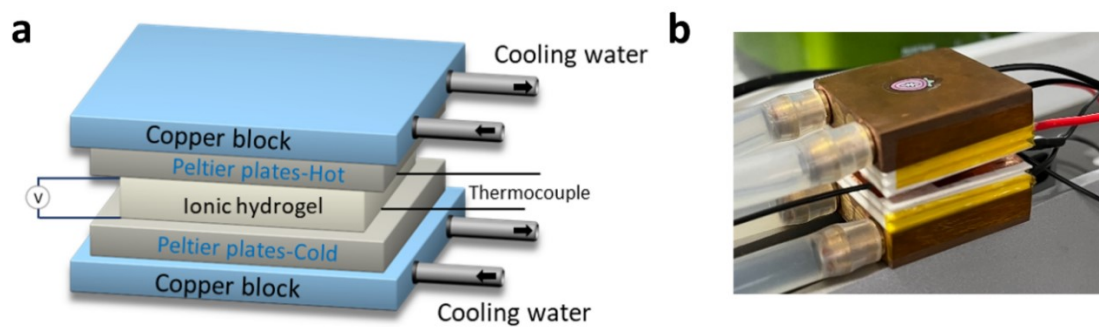


Figure S3. (a) Schematic and (b) real picture of the measurement setup for the i-TE conversion of the ionic hydrogels.

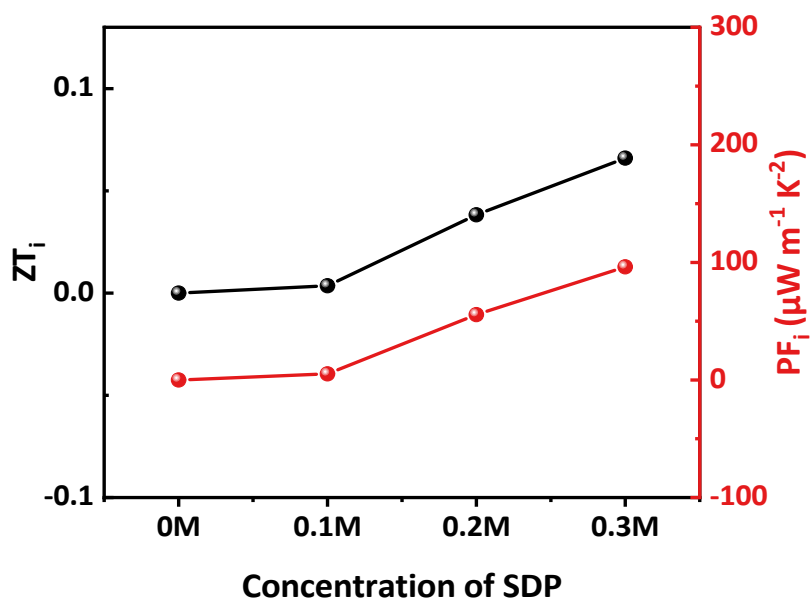


Figure S4. PF_i and ZT_i of PAA-PEO-SDP ionic hydrogels with different SDP contents.



Figure S5. Photograph of the comparison of residues of PAA-PEO-0M and PAA-PEO-0.3M ionic hydrogels after vertical combustion.



Figure S6. The screenshots from a video of wood@0M burning in an atmosphere with 42% oxygen.

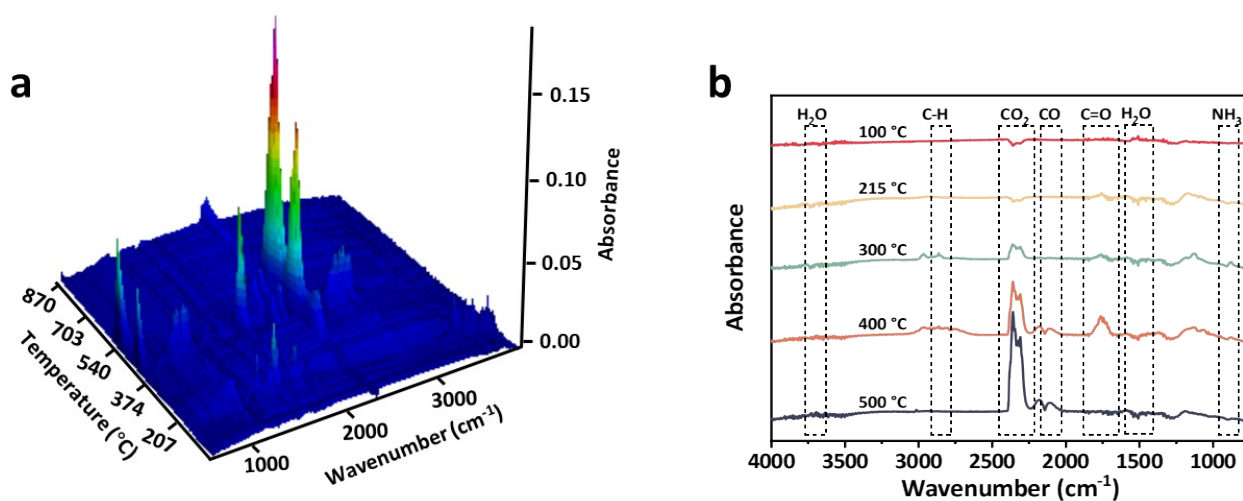


Figure S7. (a) 3D TG-FTIR spectra and (b) the corresponding FTIR spectra at different temperatures of PAA-PEO-0MSDP samples.

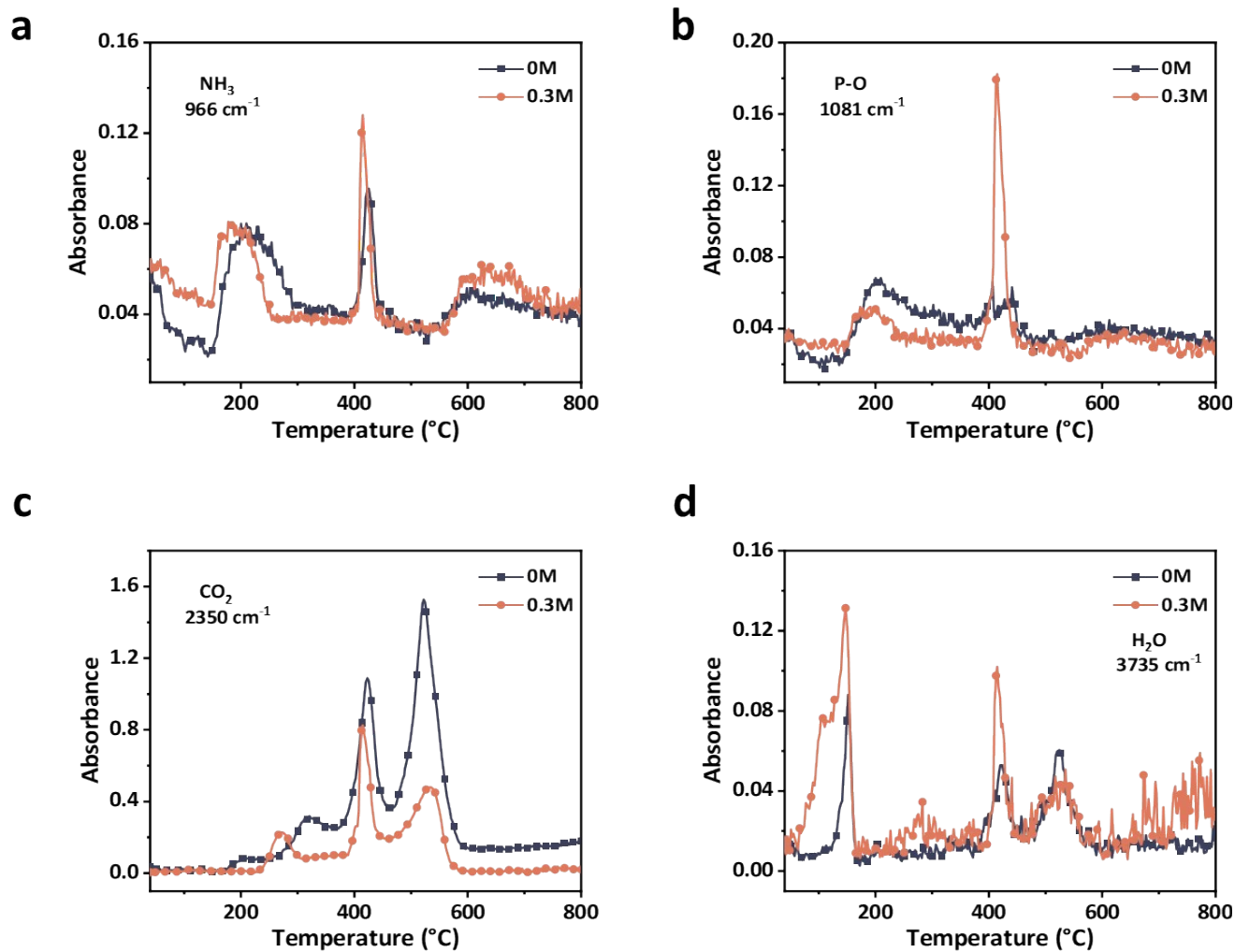


Figure S8. The absorbance curve of pyrolysis products of PAA-PEO-0M/0.3MSDP samples in air atmosphere with temperature change. (a) NH₃, (b) P-O, (c) CO₂ and (d) H₂O.

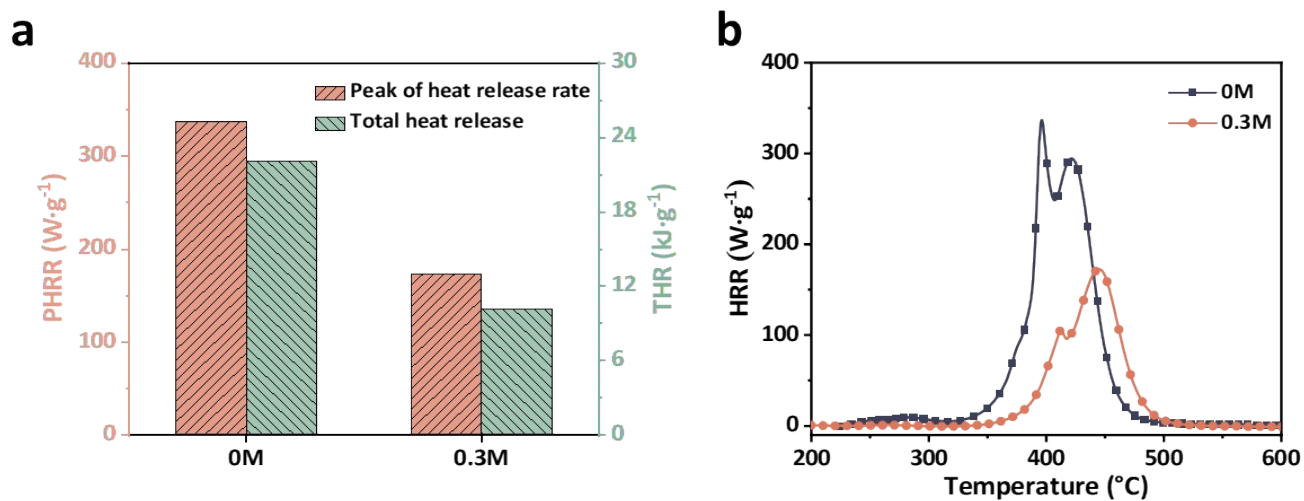


Figure S9. (a) Peak heat release rate and total heat release rate and (b) heat release rate curves for PAA-PEO-0M/0.3MSDP samples.

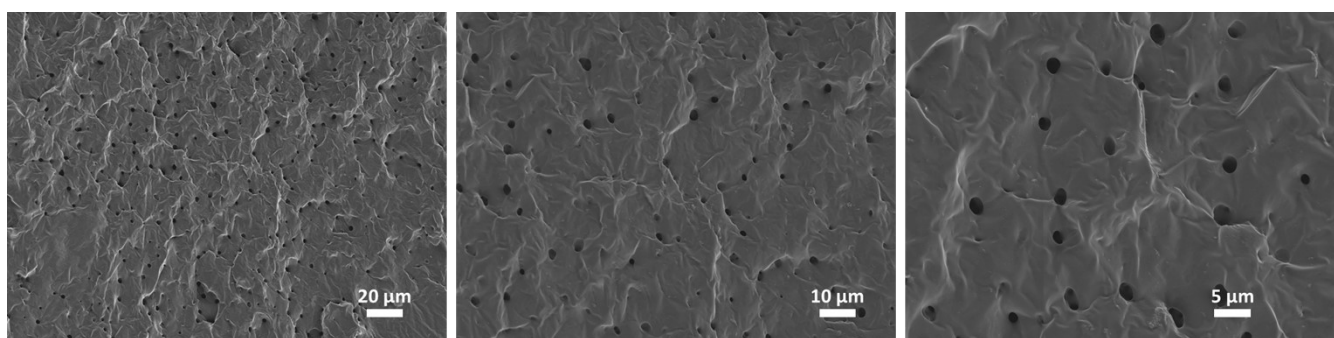


Figure S10. SEM images of PAA-PEO-0MSDP samples.

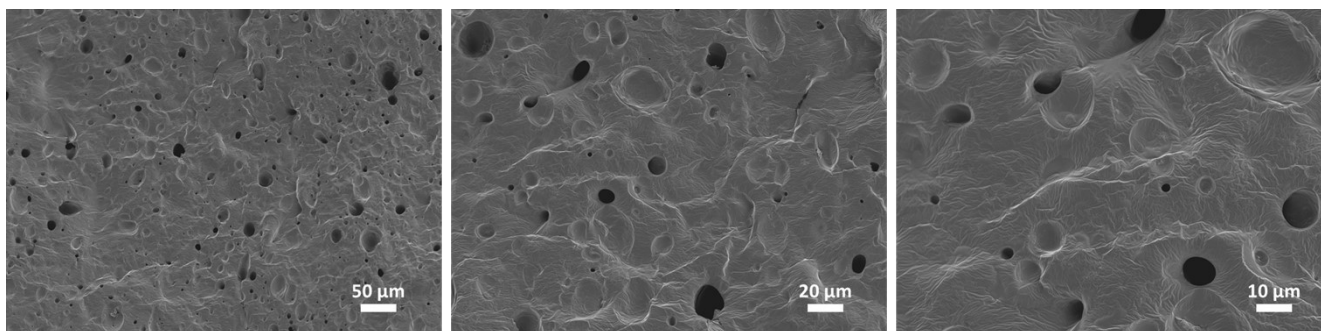


Figure S11. SEM images of PAA-PEO-0.3MSDP ionic hydrogels.

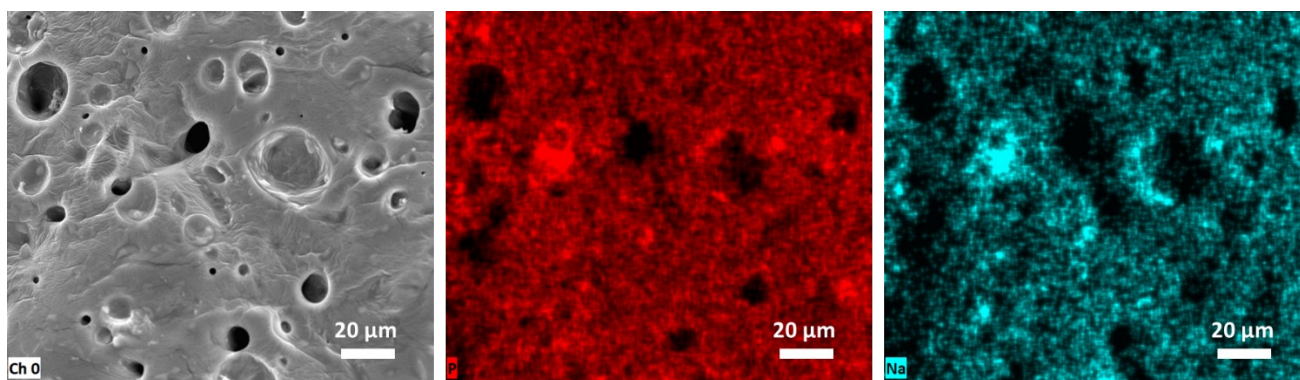


Figure S12. Mapping image of PAA-PEO-0.3MSDP ionic hydrogels.

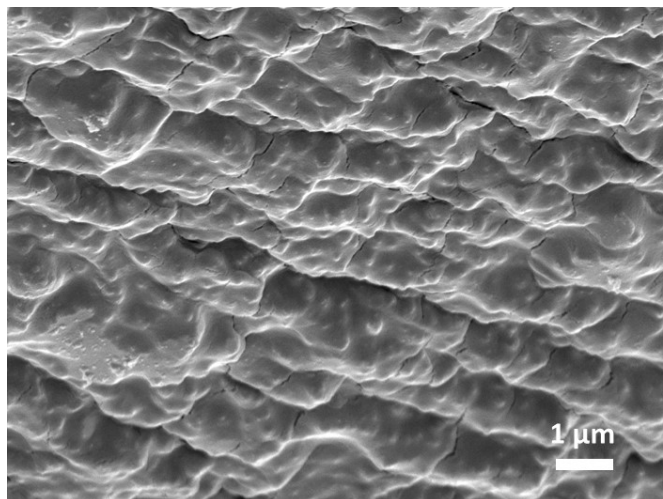


Figure S13. SEM images of PAA-PEO-0.3MSDP ionic hydrogels after burning at a larger scale.

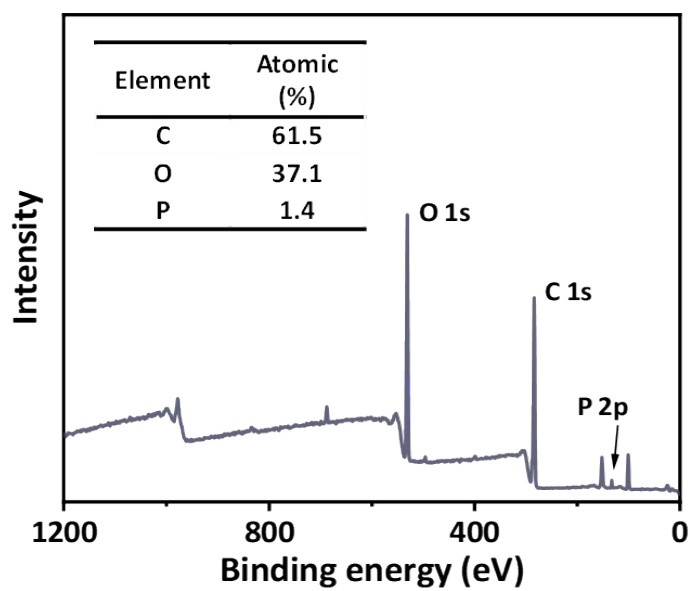


Figure S14. Total XPS spectra of the surface of PAA-PEO-0.3MSDP ionic hydrogels.

Video S1-S2.

Video S1. The fire-warning test of PAA-PEO-0MSDP ionic hydrogels.

Video S2. The fire-warning test of PAA-PEO-0.3MSDP ionic hydrogels.

References.

- [S1] Jiang, C.; Lai, X.; Wu, Z.; Li, H.; Zeng, X.; Zhao, Y.; Zeng, Q.; Gao, J.; Zhu, Y. *J. Mater. Chem. A* 2022, **10**, 21368.
- [S2] Zhao, Y.; Zeng, Q.; Jiang, C.; Lai, X.; Li, H.; Wu, Z.; Zeng, X. *Nano Energy* 2023, **116**, 108785.
- [S3] Zou, T.; Zhang, D.; Shen, K.; Huang, Z.; Xu, T.; Peng, X.; Zhang, H.; Du, Y.; Sun, L. *Adv. Compos. Hybrid Mater.* 2023, **6**, 200.
- [S4] Zou, T.; Zhang, D.; Xu, T.; Peng, X.; Zhang, H.; Du, Y. *Cellulose* 2023, **30**, 1.
- [S5] He, H.; Qin, Y.; Liu, J.; Wang, Y.; Wang, J.; Zhao, Y.; Zhu, Z.; Jiang, Q.; Wan, Y.; Qu, X.; Yu, Z. *Chem. Eng. J.* 2023, **460**, 141661.
- [S6] Zeng, Q.; Zhao, Y.; Lai, X.; Jiang, C.; Wang, B.; Li, H.; Zeng, X.; Chen, Z. *Chem. Eng. J.* 2022, **446**, 136899.
- [S7] Zeng, Q.; Wang, B.; Lai, X.; Li, H.; Chen, Z.; Xie, H.; Zeng, X. *Compos. - A: Appl. Sci. Manuf.* 2023, **164**, 107305.
- [S8] Wang, B.; Lai, X.; Li, H.; Jiang, C.; Gao, J.; Zeng, X. *ACS Appl. Mater. Interfaces* 2021, **13**, 23020.
- [S9] Xie, H.; Lai, X.; Li, H.; Gao, J.; Zeng, X. *J. Colloid Interface Sci.* 2021, **602**, 756.
- [S10] Zhao, Y.; Chen, J.; Lai, X.; Li, H.; Zeng, X.; Jiang, C.; Zeng, Q.; Li, K.; Wu, Z.; Qiu, Y. *Compos. - A: Appl. Sci. Manuf.* 2022, **163**, 107210.
- [S11] Li, H.; Ding, Z.; Zhou, Q.; Chen, J.; Liu, Z.; Du, C.; Liang, L.; Chen, G. *Nanomicro Lett.* 2024, **16**, 151.
- [S12] Xie, H.; Li, K.; Nian, J.; Zheng, J.; Lai, X.; Wu, W.; Su, X.; Wu, Y.; Zhang, X. *Compos. - A: Appl. Sci. Manuf.* 2023, **166**, 107385.